# Analysis of Spatiotemporal Distribution and Non-stationary of Extreme Precipitation Events during 1960-2018 in the Yellow River Basin

Xianglin Lv[1], Hongjing Yu[1], Hao Dong[1], Shibao Ji[1], Yaqin Qiu[1,*], Xvdong Duan[2], Hao Zheng[2]

[1]*National Key Laboratory of Basin Water Cycle Simulation and Control, China Institute of Water Resources & Hydropower Research, Beijing 100078, P. R. China*

[2]*Laboratory of Coastal Groundwater Utilization & Protection, Tianjin University of Science and Technology, Tianjin 300450, P. R. China*

Abstract:     Climate change has changed the extreme precipitation pattern in the Yellow River Basin (YRB). In this article, total of six extreme indices of rainfall were employed to assess the spatial and temporal distribution characteristics of extreme precipitation in YRB, and the GAMLSS model is applied in two typical stations (Xinghai, Yuncheng) to investigate the non-conformity in terms of persistence-CDD, intensity-R95p, and frequency-R20, respectively. The results showed that: a) In YRB, CDD had a significant upward trend, while there was a clear downward trend in R20 and SDII (Simple daily intensity index), and the spatial distribution of temporal trends varies greatly among regions, with an increasing tendency in the northwest of YRB and decreasing tendency in the southeast of YRB, which was the opposite of the spatial distribution. Indicating that rainfall decreased in the downstream of relatively wet basins, while rainfall increased in the upstream of relatively dry basins. b) Both representative stations expressed non-stationarity, but with different characteristics. In the stationary model (Model 0), the WEI (Weibull) was selected at most indices, In the non-stationary model (Model 1), the GA (Gamma) was selected at most Climate indices. In Station Xinghai in upper of YRB, drought days decreased, the mean and variance of the R20 and R95p distribution functions were increasing which indicates that the inter-annual variation became larger and more prone to extreme flooding or extreme drought. Station Yuncheng in lower of YRB also has fewer drought days, however the mean and variance of the R20 and R95p are decreasing which indicates more stable precipitation and a lower chance of extreme events than before.

## 1 INTRODUCTION

For hydrological cycle, precipitation is vital and directly affects the flood and drought events in an area. Warming leads to greater evaporation, 7% increase in air holding capacity for every 1 degree rise in temperature, more intense precipitation events would be widespread, even in places where total precipitation is reduced (Trenberth, 2011). Furthermore, precipitation change may differ in different aspects, such as totals and extremes (Donat et al., 2016). In addition, non-stationarity has been widely reported in hydrological time series analysis, and related studies have shown that rainfall series also exhibit non-stationary characteristics (Zhang et al., 2016; Gu et al., 2019; Wu et al., 2021; Medeiros

et al., 2019). Consequently, research about the spatiotemporal dynamics of extreme precipitation and its distribution pattern under the changing environment is significant for the monitoring and prevention of climate disasters like floods and droughts (Zou et al., 2021).

For the latest years, the dynamic changes of spatial and temporal variability and non-stationarity of extreme precipitation has attracted the attention of many scholars. Gao et al. (2018) used six climate variables based on GAMLSS showing the existence of non-stationarity in the Coastal areas of Southeast China. Lei et al. (2021) pointed out the intensity indices (PRCPTOT, SDII, R99P) and frequency indices (R20, R10) of extreme precipitation showed stationary characteristics, however the duration indices (CWD, CDD) showed non-stationary

characteristics in the Poyang Lake Basin of China. Hao et al. (2019) used two precipitation indices (RX5day, R20) which choose two covariates, time and climate, to determine the non-stationarity of extreme precipitation in the Han River basin of China. Liu et al. (2008) shows that precipitation is significantly correlated with longitude and not with latitude, and exhibits a downward trend at most stations in the YRB. S Swain et al., showed that annual rainfall has increased by 10.65% from 1901-2002 by Sen's slope and Mann-Kendall (M-K) test (Swain et al., 2019). He et al., used M-K method to analyze the temporal trends of extreme rainfall index in YRB from 1960 to 2012, and its spatial distribution (He & He, 2014). Yang et al. (2017) pointed out that the frequency of extreme precipitation exists significant increasing trends by POT sampling method.

Existing studies have been concentrating on the Spatiotemporal patterns of extreme rainfall indices and their effects. This research adopts the Modified Mann-Kendall (MM-K) method to compensate for the shortcomings of autocorrelation in the MK test, and establishes the GAMLSS model with time as the independent variable to investigate the change of the distribution function of extreme rainfall index in YRB.

## 2 STUDY AREA AND DATA COLLECTION

YRB is located in the arid and semi-arid regions (between 96°-116°E and 32°-42°N), arid in the west, wet in the east, dry in winter and dry in spring, rainy in summer and autumn. YRB has an important influence in northern China (Fig 1.). YRB has a huge difference in elevation from east to west, and the geomorphology varies greatly between different regions. In addition, it is in the mid-latitude zone, which is affected by atmospheric circulation and monsoon circulation in a complex way, and the climate varies significantly in different areas of YRB. The data used were obtained from the daily precipitation data of 874 stations from 1960 to 2018 provided by the China Meteorological Science Data Sharing Service, including 91 precipitation stations in the Yellow River basin, and the location of precipitation stations is shown in Figure 1. To ensure the continuity and uniformity of the precipitation data, only the years with continuous measured data were included. Secondly, all data were checked for outliers to ensure data integrity and accuracy.
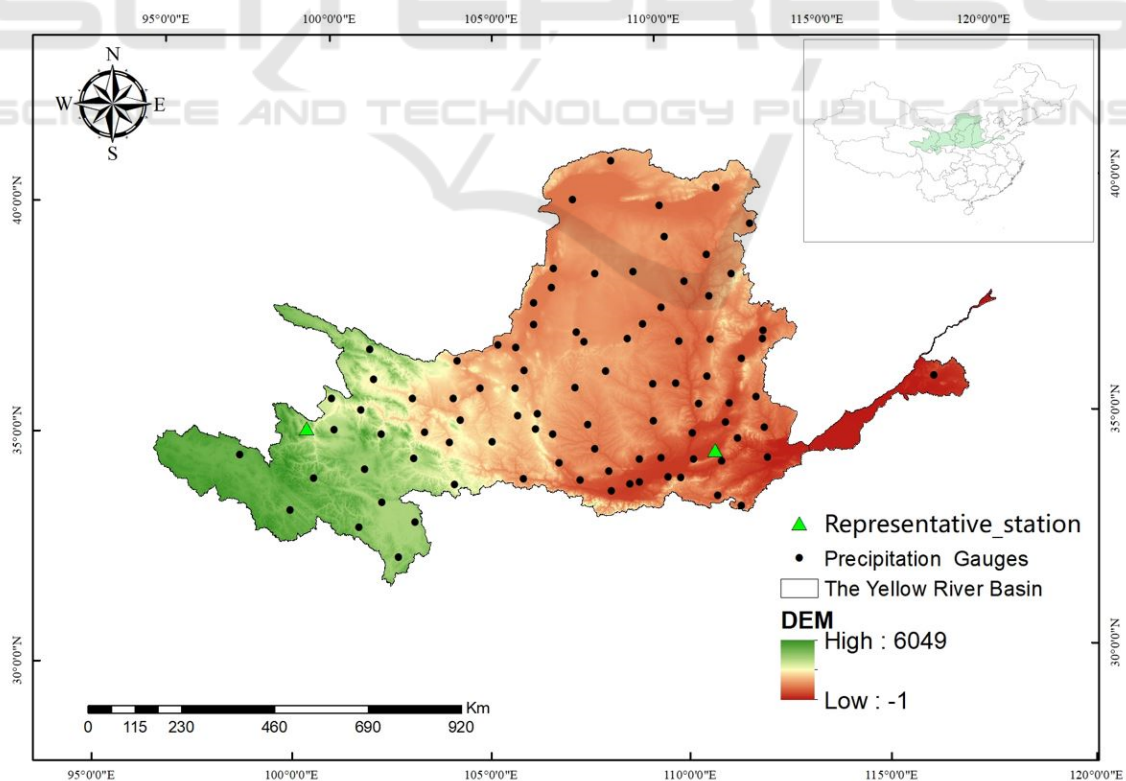


Figure 1: Location of meteorological stations and study area.

## 3 METHODS

### 3.1 Extreme Precipitation Index

Six extreme precipitation indices were selected from the 27 extreme climate indices recommended by the Expert Group on Climate Change Monitoring and

Indicators jointly established by WMO, Commission for Climatology (CCI) and other meteorological organizations (Costa & Soares, 2009), as shown in Table 1. All extreme precipitation indices were calculated using RClimate software.

Table 1: Definition of extreme precipitation indices.

| Index | Name | Definition | Unit |
|---|---|---|---|
| SDII | Simple daily intensity index | Annual total precipitation divided by the number of wet days (defined as PRCP>=1.0mm) in the year | mm/d |
| PRCPTOT | Annual total wet-day precipitation | Annual total PRCP in wet days (Rain Rate (RR)>=1mm) | mm |
| R95P | Very wet days | Annual total PRCP when RR>95th percentile | mm |
| CDD | Consecutive dry days | Maximum number of consecutive days with RR<1mm | d |
| R10 | Number of heavy precipitation days | Annual count of days when PRCP>=10mm | d |
| R20 | Number of very heavy precipitation days | Annual count of days when PRCP>=20mm | d |

### 3.2 MM-K Trend Analysis Method

The M-K test is an important nonparametric trend test for time series, which is widely used in the field of hydrological statistics because it does not require the series to be examined to obey a certain probability distribution, overcoming the problems of bias, non-identical distribution, and having outliers in hydrological data. Although the MK method has the advantages of nonparametric tests, it does not solve the problem of data independence required in statistical tests of hydrological series (Zhang et al.,

2013). Hamed and Rao (1998) proposed a Modified Mann-Kendall test which corrected V (S) by using the effective sample size (ESS), which reflects the effect of serial autocorrelation on the test results (Tian et al., 2017). Swain et al. (2021) showed a significantly increasing trend of drought in Narmada River Basin. The corrected V (S) equation is as follows:

$$V^*(S) = V(S)\frac{n}{n^*} \quad (1)$$

$$\frac{n}{n^*} = 1 + \frac{2}{n\,(n-1)\,(n-2)} \sum_{j=1}^{n-1} (n-k)\,(n-k-1)\,(n-k-2)r_k^R \quad (2)$$

$$r_k = \frac{\frac{1}{n-k}\sum_{t=1}^{n-k}[X_t - E(X_t)][X_{t+k} - E(X_t)]}{\frac{1}{n}\sum_{t=1}^{n}[X_t - E(X_t)]^2} \quad (3)$$

$$E(X_t) = \frac{1}{n}\sum_{t=1}^{n} X_t \quad (4)$$

### 3.3 GAMLSS Model

The GAMLSS model is a generalizable additive model based on the location parameter, scale parameter and shape parameter (Rigby & Stasinopoulos, 2005). It extends the form of the assumption of the distribution from exponential distribution to a more generalized form, which can be parametric or nonparametric model for the location parameter, scale parameter and shape parameter of a distribution simultaneously under

various distribution assumptions, describing the linear or nonlinear relationship between any statistical parameter of the sequence of random variables and the explanatory variables (Zhang et al., 2015; Zhang et al., 2014). Then the regression relationship between the distribution factors, explanatory variables, and random effects are as follows:

$$g_k(\theta_k) = X_k\beta_k + \sum_{j=1}^{m} h_{jk}(x_{jk}) \quad (5)$$

Where $g_k$ is the monotonic connection function; $\theta_k$ is the vector of k distribution parameter with length n; $X_k$ is the explanatory variable in the n ×m matrix; $\beta_k$ is the parameter vector of length m; and $h_{jk}$ (.) represents the joint function (the cubic

spline function is applied here) between the distribution parameters and explanatory variables $x_{jk}$.

The linear function and cubic spline function are chosen as the parameter to explain the function of association between variables. Five distributions, lognormal (LOGNO), gamma (GA), normal (NO), Weibull (WEI) and logistic (LO), were applied to model the extreme precipitation data. The Akaike Information Criterion (AIC) was used to penalize overfitting of the models and to select the best model (Arnold, 2010). The best model fit is evaluated by snail plot and the independence and normality of the residuals are checked.

# 4 RESULTS

## 4.1 Temporal Variation of Extreme Precipitation Characteristics in the Yellow River Basin

According to the daily data from 91 precipitation stations in YRB, a total of six extreme precipitation indices, CDD, PRCPTOT, R10, R20, R95P and SDII, were calculated for each precipitation station year by year, and the Thiessen polygon method was used to calculate the extreme precipitation indices. The MMK test results for these indices are presented in Table 2.

Table 2: MMK trend results.

|       | trend      | h     | z-value | slope | intercept | mean   |
|-------|------------|-------|---------|-------|-----------|--------|
| CDD   | decreasing | TRUE  | -4.49   | -1.08 | 101.34    | 85.55  |
| PTOT  | no trend   | FALSE | -0.66   | -0.34 | 579.37    | 568.45 |
| R10   | no trend   | FALSE | 0.16    | 0.005 | 15.78     | 15.92  |
| R20   | increasing | TRUE  | 2.03    | 0.02  | 5.20      | 5.58   |
| R95P  | no trend   | FALSE | -0.90   | -0.36 | 142.21    | 134.80 |
| SDII  | increasing | TRUE  | 2.83    | 0.02  | 7.30      | 7.34   |

As shown in Figure 2, CDD, PRCPTOT, and R95P showed a decreasing trend, and R10, R20, and SDII showed an increasing trend and slope of -1.08/a (CDD), -0.34mm/a (PRCPTOT), 0.005mm/a (R10), 0.02mm/a (R20), - 0.36mm/a (R95P), and 0.02mm/a (SDII). The decreasing trend of CDD was significant (Z=-4.49), and the increasing trend of R20 (Z=2.03) and SDII (Z=2.83) was significant. Hence the trend of drought is decreasing, and precipitation distribution is more homogeneous in annual basis. Daily precipitation intensity showed a significant increasing trend, while annual precipitation showed a non-significant decreasing trend. In contrast, R20 shows a significant increasing trend and R10 shows a non-significant increasing trend, indicating that the frequency of extreme precipitation in YRB in recent years is dominated by moderate and heavy rainfall, and the precipitation process is more concentrated.

From Figure 3, the number of CDD in YRB basin showed a decreasing trend, with the most drastic decrease in the northwestern and northeastern parts of YRB, the trend of PRCPTOT is increasing in the northwestern part of the basin. In the southern parts of the basin, the number of consecutive dry days decreased the least, the number of wet days increased the least, and the PRCPTOT was also in a decreasing trend and more significant.

The number of light rain days, R10, was on a decreasing trend in the central, southern, and eastern parts of the study area. The trend in the northwest is consistent with that of PRCPTOT, but differs in the Yellow River source area, where the annual precipitation increases, and the number of light rain days R10 shows a decreasing trend and the number of medium rain days R20 shows an increasing trend.

Compared with PRCPTOT and R10, R20 and R95P also showed an increasing trend in the middle part of YRB, indicating that the decrease in annual precipitation in the middle part of YRB was mainly caused by the decrease in the number of light rain days, and the number of medium rain days showed an increasing trend in contrast to the decrease in annual precipitation. The increase in the frequency of moderate and heavy rainfall somewhat suppressed the decrease in annual precipitation caused by the decrease in light rainfall.

## 4.2 Spatial Distribution of Extreme Precipitation in the Yellow River Basin

From Figure 4, significant differences could be found in different regions of YRB, the CDD values range from 40.2-147.6, PRCPTOT ranges from

155.4-1144, light rain days between 4.716-29.59, medium rain days between 0.679-17.38, R95P between 39.96-73.38, and SDII between 3.27-15.95.

In the study area, except for SDII, the multi-year average of extreme precipitation indices basically shows a distribution characteristic of gradually increasing from northwest to southeast, and SDII shows a distribution characteristic of gradually increasing from west to east. The results are consistent when comparing the spatial distribution of Yang Peiyu using POT sampling with 95% quantile as the threshold.
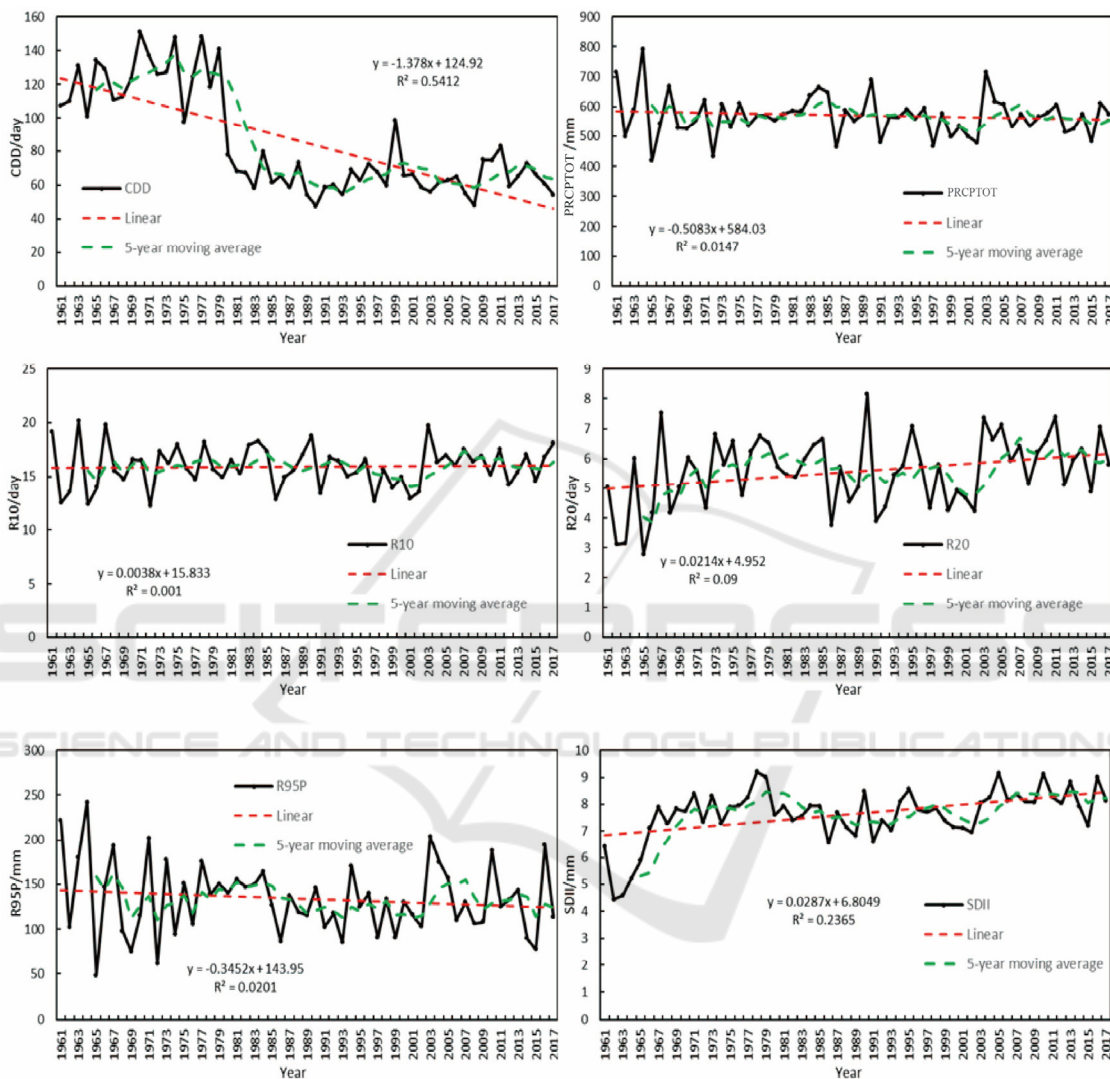


Figure 2: Time series of extreme precipitation index in YRB.

## 4.3 Non-stationary Analysis of Extreme Precipitation in YRB

From the upper and lower reaches of YRB, two stations (Xinghai, Yuncheng) were selected as the representative stations for non-stationarity analysis. Three indices were selected from six extreme climate indices as mentioned in preceding part of the paper. These are Consecutive dry days (CDD) that can describe the persistence of extreme precipitation events, the number of very heavy rainfall days (R20) which can describe the frequency of extreme precipitation events, the Very wet days (R95p) which can indicate the intensity of extreme precipitation events.
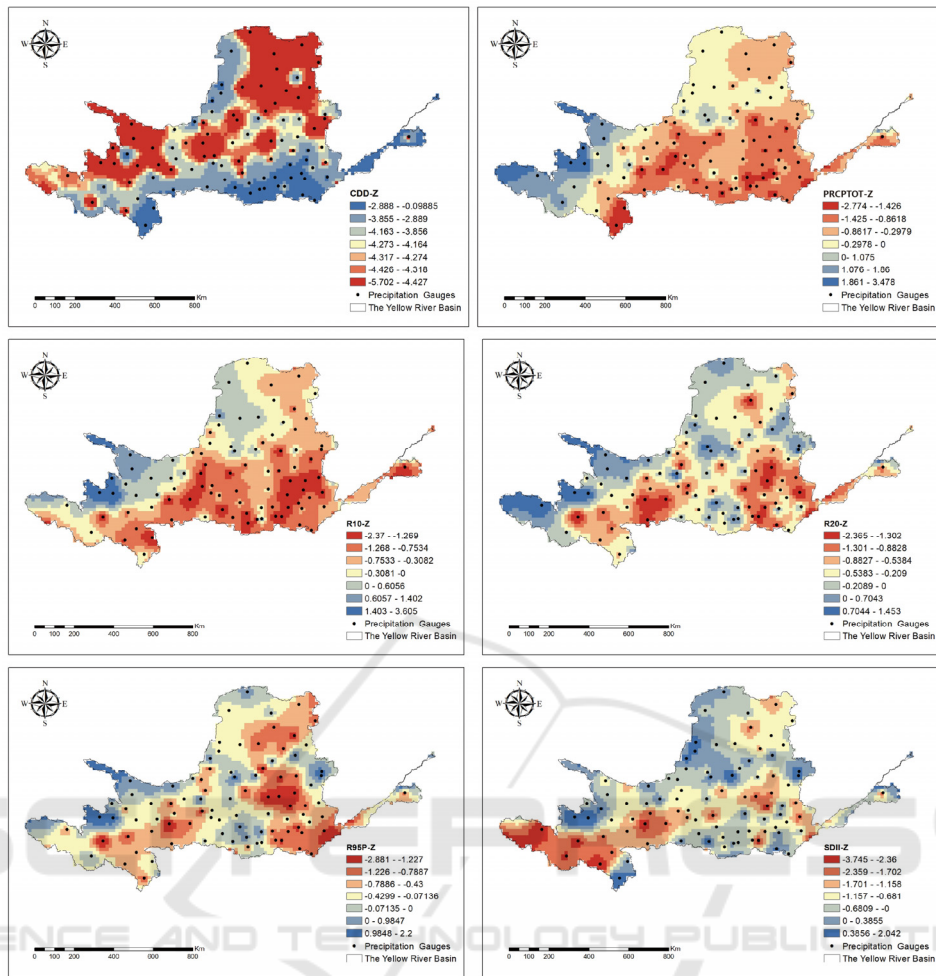
Figure 3: Spatial distribution of MMK test results in the Yellow River Basin.

Based on the AIC values, one distribution with the best fit was selected for each site. (from Table 3). In the Model 0, the WEI was selected at most indices (4 indices), GA and LOGNO performed best at one

Indexes. In the Model 1, the GA was selected at most Climate indices (4 indices), NO and WEI performed best at one index.

Table 3: Summary for the fitted models with time as the covariate: cs () indicates the dependence is via the cubic splines; and ct refers to a parameter that is constant.

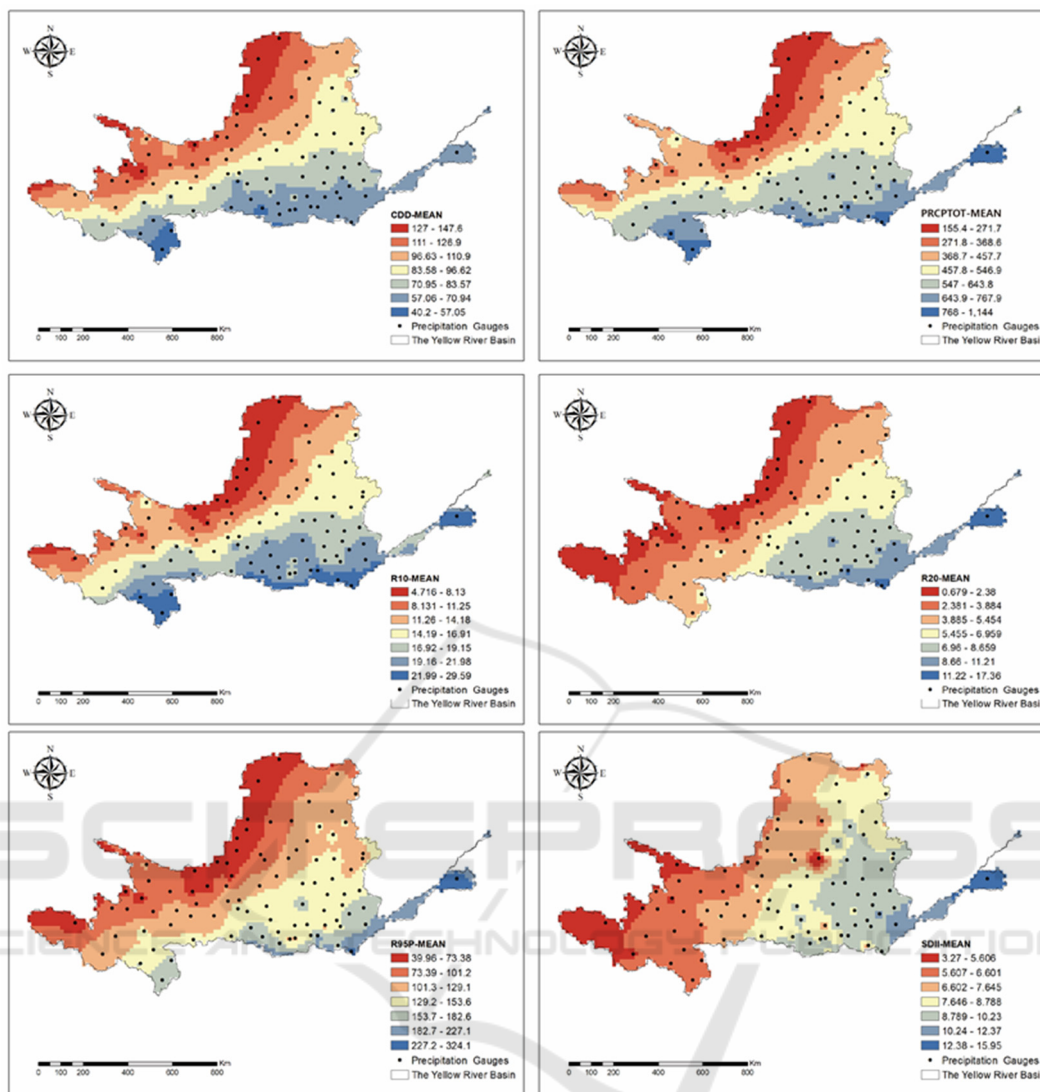| | | Model 0 | | Model 1 | | | |
|---|---|---|---|---|---|---|---|
| Extreme Index | | Distribution | AIC | Distribution | $\theta_1$ | $\theta_2$ | AIC |
| Xinghai | CDD | WEI | 630.3423 | NO | cs (t,3) | ct | 596.2364 |
| | R95p | WEI | 628.8753 | WEI | cs (t,0) | cs (t,2) | 622.2544 |
| | R20 | GA | 192.6919 | GA | cs (t,3) | ct | 189.9838 |
| Yuncheng | CDD | LOGNO | 571.527 | GA | ct | cs (t,0) | 565.378 |
| | R95p | WEI | 697.5988 | GA | cs (t,0) | cs (t,2) | 697.0961 |
| | R20 | WEI | 309.0856 | GA | ct | cs (t,2) | 308.5433 |

Figure 4: Spatial distribution of extreme precipitation in the YRB.

Model 0 is a steady-state model with constant mean and variance, and Model 1 is a non-stationary model with varying mean and variance which time is covariate). The smaller AIC values for the non-stationary model 1 compared to the stationary model 0 suggest that the non-stationary model 1 indicates that the model with time as a covariate performs better than the model with constant parameters. From table 3, the parameter $\theta_1$ is the cubic spline function with degree of freedom 3 and the parameter $\theta_2$ is constant in Xinghai-CDD and Xinghai-R20. The parameter $\theta_1$ is constant and the parameter $\theta_2$ is the cubic spline function with degree of freedom 3 in Yuncheng-CDD and Yuncheng-R20. The parameter $\theta_1$ is linear trend function and the parameter $\theta_2$ is the

cubic spline function with degree of freedom 2 in Xinghai-R95p and Yuncheng-R95p.

Figure 5, whose vertical coordinate is the normal normalized residual series, and the horizontal coordinate is the theoretical residual value, shows the worm plot of the residuals of the optimal model for each index, and the red line in the middle is a cubic polynomial curve fitted by the series of scatter points in the plot. All the scatter points in the worm plot lie within the confidence interval between the upper and lower curves. The above fitting results show that the residual series of the optimal model for each site can be considered to obey the standard normal distribution, and thus the distribution type and parameter selection of each preferred model

500

constructed earlier can be judged to be reasonable.

Based on the distribution and parameters of each preferred model, the quantile values corresponding to each indicator series at the specified time and at the specified percentile can be calculated. Figure 6 shows the quantile plot for each indicator series, where the dots represent the measured values for each year at the site, and the solid lines of different

colors represent the quantile values corresponding to the five percentiles of 5%, 25%, 50%, 75%, and 95%, respectively. Most of the data points are between 5% and 95% of the quantile curve. It indicates that the simulation results of the theoretical distribution of each station match well with the distribution of the actual measured points.
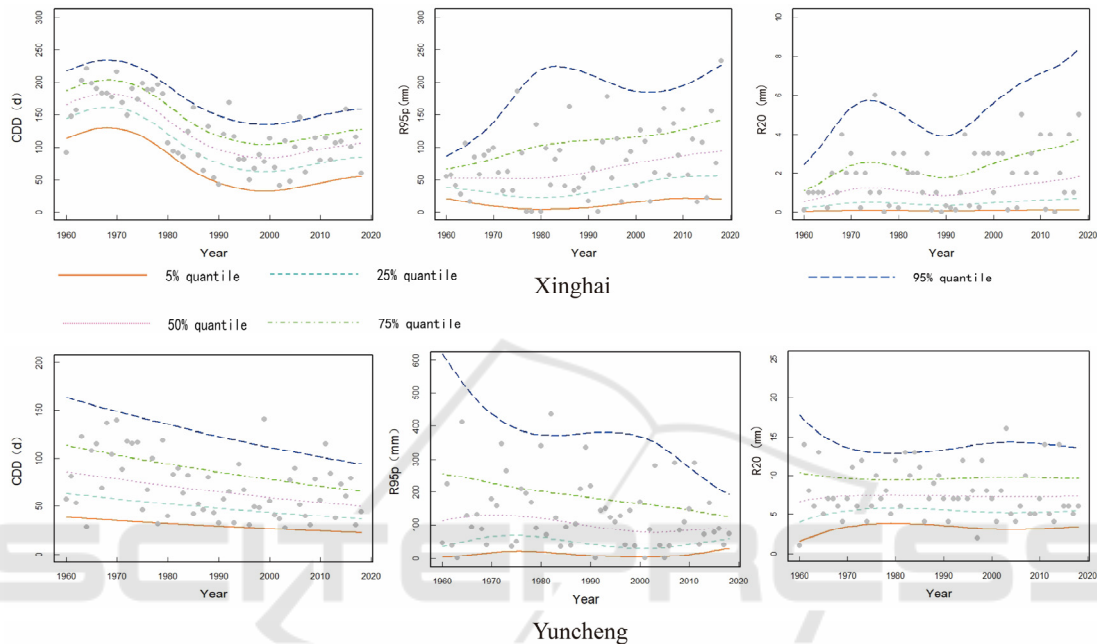


Figure 5: The residual worm diagram of the optimal model.

In terms of persistence of dry day (CDD), the parameter $\theta_1$ related to the mean value of the extreme precipitation events has a nonlinear decreasing trend in station Xinghai, the parameter $\theta_2$ related to the fluctuation of the extreme precipitation events has no significant trend in station Xinghai. The parameter $\theta_1$ is on a linear decreasing trend in station Yuncheng, The parameter $\theta_2$ also has a linear decreasing trend in station Yuncheng.

In terms of intensity (R95p), the parameter $\theta_1$ is on a nonlinear decreasing trend in station Xinghai, the parameter $\theta_2$ has a nonlinear increasing trend in station Xinghai. The parameter $\theta_1$ is on a nonlinear decreasing trend in station Yuncheng, the parameter $\theta_2$ also has a nonlinear decreasing trend in station Yuncheng.

In terms of frequency (R20), the parameter $\theta_1$ is on a nonlinear increasing trend in station Xinghai, the parameter $\theta_2$ also has a nonlinear increasing trend in station Xinghai. The downward trend of parameter $\theta_1$ is non-significant in station Yuncheng, the upward

of parameter $\theta_2$ is non-significant in station Yuncheng.

# 5 CONCLUSION

In this paper, we analyzed the spatiotemporal variation of six extreme precipitation indices in the YRB from 1960 to 2018 by MMK trend test and selected three indices in terms of persistence (CDD), frequency (R20) and intensity (R95p) for non-stationary analysis through GAMLSS model.

In YRB, CDD has a significant upward trend, R20 and SDII have a significant downward trend, and other indicators have no significant changes. In addition, the spatial distribution of temporal trends varies considerably between regions, with an upward trend in the northwest and a downward trend in the southeast. However, the spatial distribution of the multi-year average values of the basin precipitation indices shows an opposite trend which gradually

increases from northwest to southeast. Rainfall decreases in the relatively wet downstream portion of basin and increases in the relatively dry upstream portion of basin, the gap between upstream and downstream will gradually decrease.

In the Model 0, the WEI performed best at most indices (4 indices), GA and LOGNO performed best at one index. In the Model 1, the GA performed best at most Climate indices (4 indices), NO and WEI performed best at one index. In Station Xinghai in

upper parts of YRB, decreasing drought days, along with the increasing mean and variance of the R20 and R95p distribution functions with time indicates that the inter-annual variation became larger and more prone to extreme flooding or extreme drought. Station Yuncheng in lower of YRB also has fewer drought days, however the mean and variance of the R20 and R95p are decreasing which indicates more stable precipitation and a lower chance of extreme events than before.
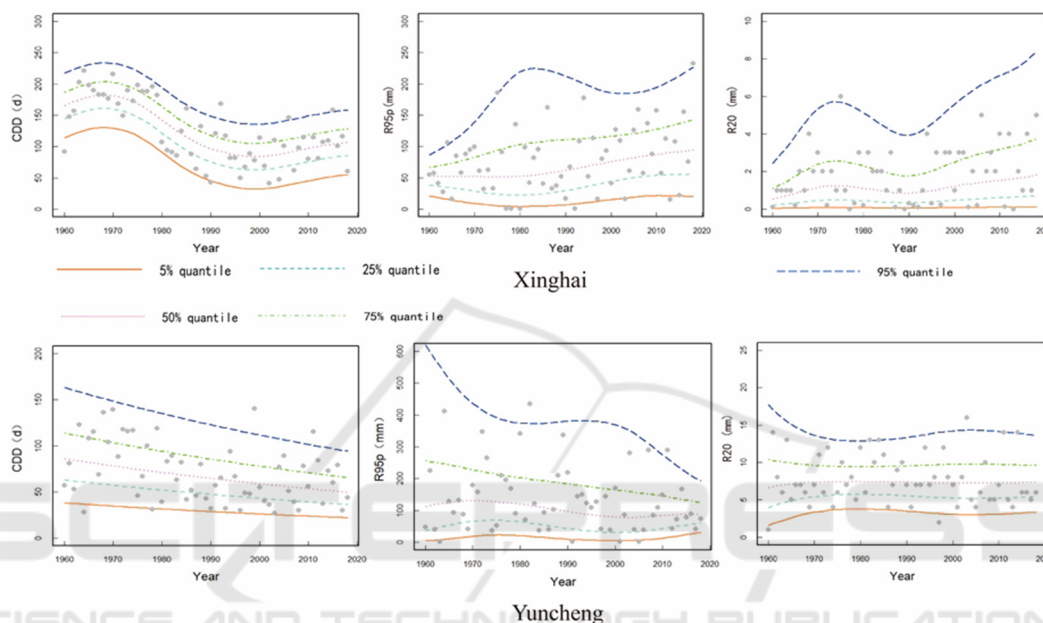


Figure 6: 5%, 25%, 50%, 75% ,95%for two representative stations CDD, R95p, R20. 95% quantile.

## REFERENCES

Arnold, T. W. (2010). Uninformative parameters and model selection using Akaike's Information Criterion. *The Journal of Wildlife Management*, *74*(6), 1175-8.

Costa, A. C., & Soares, A. (2009). Trends in extreme precipitation indices derived from a daily rainfall database for the South of Portugal. International Journal of Climatology, A Journal of the Royal *Meteorological Society*, *29*(13), 1956-75.

Donat, M. G., Lowry, A. L., Alexander, L. V., O'Gorman, P. A., & Maher, N. (2016). More extreme precipitation in the world's dry and wet regions. *Nature Climate Change. 6*(5), 508-13.

Gao, L., Huang, J., Chen, X., Chen, Y., & Liu, M. (2018). Contributions of natural climate changes and human activities to the trend of extreme precipitation. *Atmospheric Research*, *205*, 60-9.

Gu, X., Zhang, Q., Li, J., Singh, V. P., & Sun, P. (2019). Impact of urbanization on non-stationarity of annual and seasonal precipitation extremes in China. *Journal of Hydrology*, *575*, 638-55.

Hamed, K. H., & Rao, A. R. (1998). A modified Mann-Kendall trend test for autocorrelated data. *Journal of Hydrology*, *204*(1-4), 182-196.

Hao, W., Shao, Q., Hao, Z., Ju, Q., Baima, W., & Zhang, D. (2019). Non-stationary modelling of extreme precipitation by climate indices during rainy season in Hanjiang River Basin, China. *International Journal of Climatology*, *39*(10), 4154-69.

He, Z., & He, J. (2014). Temporal and spatial variation of extreme precipitation in the Yellow River Basin from 1960 to 2012. *Resources science*, *36*(3), 490-501.

Rigby, R. A., & Stasinopoulos, D. M. (2005). Generalized additive models for location, scale and shape. *Journal of the Royal Statistical Society*, *54*, 507-554.

Lei, X. Y., Gao, L., Ma, M. M., Dang, H. F., & Gao, J. Y. (2021). Temporal-spatial and non-stationarity characteristics of extreme precipitation in the Poyang Lake Basin, China [J/OL]. *Chinese Journal of Applied Ecology*, *2021*, 1-11.

Liu, Q., Yang, Z., & Cui, B. (2008). Spatial and temporal variability of annual precipitation during 1961–2006 in Yellow River Basin, China. *Journal of hydrology*, *361*(3-4), 330-8.

Medeiros, E. S., de Lima, R. R., Olinda, R. A., Dantas, L. G., & Santos, C. A. (2019). Space–Time Kriging of Precipitation, Modeling the Large-Scale Variation with Model GAMLSS. *Water*, *11*(11), 2368.

Swain, S., Mishra, S. K., & Pandey, A. (2021). A detailed assessment of meteorological drought characteristics using simplified rainfall index over Narmada River Basin, India. *Environmental Earth Sciences*, *80*(6), 221.

Swain, S., Dayal, D., Pandey, A., & Mishra, S. K. (2019). Trend analysis of precipitation and temperature for Bilaspur District, Chhattisgarh, India. In World Environmental and Water Resources Congress 2019, Groundwater, Sustainability, Hydro-Climate/Climate Change, and Environmental Engineering (pp. 193-204). Reston, VA, American Society of Civil Engineers.

Tian, J., Liu, J., Wang, J., Li, C., Nie, H., & Yu, F. (2017). Trend analysis of temperature and precipitation extremes in major grain producing area of China. *International Journal of Climatology*, *37*(2), 672-87.

Trenberth, K. E. (2011). Changes in precipitation with climate change. *Climate Research*, *47*(1-2), 123-38.

Wu, X., Meng, F., Liu, P., Zhou, J., Liu, D., Xie, K., Zhu, Q., Hu, J., Sun, H., & Xing, F. (2021). Contribution of the Northeast Cold Vortex Index and Multiscale Synergistic Indices to Extreme Precipitation Over Northeast China. *Earth and Space Science*, *8*(1), e2020EA001435.

Yang, P. Y., Zhang, Q., Shi, P. J., Gu, X. H., & Li, Q. (2017). Spatiotemporal Distribution of Precipitation Extremes and Related Implications Across the Yellow River Basin, China. *Journal of Wuhan University: Science Edition*, *63*(4), 368-376.

Zhang, D. D., Yan, D. H., & Wang, Y. C. (2015). GAMLSS-based nonstationary modeling of extreme precipitation in Beijing–Tianjin–Hebei region of China. *Natural Hazards*, *77*, 1037–1053.

Zhang, D. D., Lu, F., Zhou, X. N., Chen, F., Geng, S. M., & Guo, W. (2016). GAMLSS model-based analysis on non-stationarity of extreme precipitation in Daduhe River Basin. *Water Resources and Hydropower Engineering*, *47*(05), 12-15+20.

Zhang, D. W., Cong, Z. T., & Ni, G. H. (2013). Comparison of three Mann- Kendall methods based on the China's meteorological data. *Advances in Water Science*, *24*(4), 490-496.

Zhang, Q., Gu, X. H., Singh, V. P., Xiao, M. Z., & Xu, C. Y. (2014) Stationarity of annual flood peaks during 1951-2010 in the Pearl River basin, China. *Journal of Hydrology*, *519*, 3263–3274.

Zou, L., Yu, J. Y., Wang, F. Y., & Zhang, Y. (2021). Spatial-temporal variations of extreme precipitation indices and their response to atmospheric circulation factors in the Weihe River Basin. *Arid Zone Research*, *38*(3), 764-774.